EUROPHYSICS LETTERS 10 May 1997

Europhys. Lett., **38** (5), pp. 389-394 (1997)

Inhomogeneous structure formation and shear-thickening in worm-like micellar solutions

P. Boltenhagen[1](*), Yuntao Hu[2], E.F. Matthys[2] and D.J. Pine[1,3]

[1] *Department of Chemical Engineering, University of California, Santa Barbara, CA 93106, USA*
[2] *Department of Mechanical Engineering, University of California, Santa Barbara, CA 93106, USA*
[3] *Department of Materials, University of California, Santa Barbara, CA 93106, USA*

(received 6 January 1997; accepted in final form 1 April 1997)

PACS. 83.50.By– Transient deformation and flow; time-dependent properties.
PACS. 83.50.Qm– Thixotropy; thickening flows.

Abstract. – The time evolution of flow-induced structures in low-concentration worm-like micellar solutions is studied using direct visualization and rheological methods. The visualization measurements show growth of a new viscous shear-induced phase (SIP) starting on the inner wall of a Couette shear cell at a time t_1 after the commencement of shear flow. The SIP continues to grow across the shear cell until it fills the entire gap at a time t_2. Rheological measurements show that the time t_1 corresponds to the induction time for the increase in stress and that t_2 corresponds to the plateau time for the saturation of stress. These measurements provide convincing evidence that the increase of stress with time results from the inhomogeneous growth of a new shear-induced phase in the flow cell. The growth of the new phase across the cell is approximately linear in time.

Introduction. – Surfactant molecules are comprised of mutually insoluble sub-structures, generally one hydrophilic head and one or more hydrophobic tails. The introduction of such molecules into water at concentrations above the critical micelle concentration leads to the formation of aggregates where the hydrophobic tails are separated from water by a barrier made with the heads. Because of the self-assembling nature of surfactant molecules, micellar solutions may undergo structural changes when subjected to flow and thus exhibit unusual rheological behavior. As early as 40 years ago, Nash observed that eddies produced by stirring were rapidly destroyed in an aqueous solution of cationic surfactant molecules [1]. However, quantitative studies of the rheology of surfactant solutions started only about 15 years ago [2]. One of the most perplexing phenomena is the shear thickening and rheopexy observed in a wide class of low-concentration worm-like micellar solutions. These solutions exhibit a steep increase of viscosity as the shear rate is increased above a critical value, but the increase occurs

(*) Permanent address: Laboratoire d'Ultrasons et de Dynamique des Fluides Complexes, URA au CNRS no. 851, Université Louis Pasteur – 4 rue Blaise Pascal, 67070 Strasbourg, France.

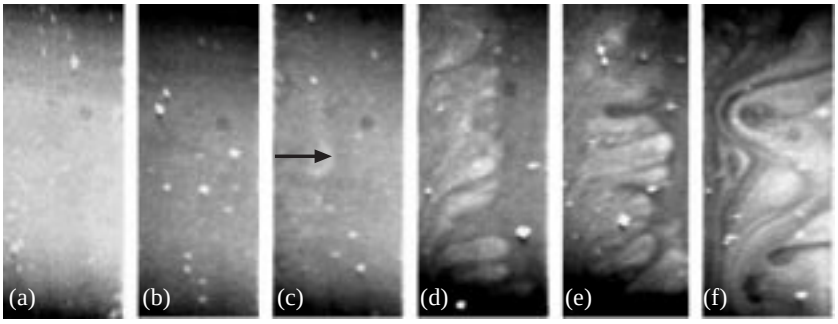

Fig. 1. – Images of the growth of the SIP as a function of time after the commencement of shear flow for $\dot{\gamma} = 60\ \mathrm{s}^{-1}$. The inner wall of the Couette cell is on the left-hand side of each image; the outer wall is on the right hand side. (a) $t = 0$ s. The homogeneous solution at equilibrium prior to the commencement of shear flow. (b) $t = 1$ s. Just after the commencement of shear flow. The decrease in scattering results from the rapid alignment of micelles with the flow direction. (c) $t = 62$ s. The SIP, faintly visible on left-hand side, has grown from the inner cylinder to fill about 35% of the cell. The arrow shows the extent of the growth of the cell. (d) $t = 125$ s. The SIP, now clearly visible, fills approximately 60% of the cell. Note the densely packed finger-like structure of the SIP. (e) $t = 140$ s. The SIP fills approximately 80% of the cell. (f) $t = 159$ s. The SIP fills the entire cell. The ongoing shear flow results in the continuous breaking and reforming of the SIP leading to complex structures and flow patterns.

slowly, often taking minutes to achieve a steady-state value. Most of the worm-like micellar systems which exhibit these phenomena consist of aqueous solutions of cationic surfactants (*e.g.*, CTAB) with a strongly bound counterion (*e.g.*, sodium salicylate). It has been proposed that these phenomena are caused by some type of shear-induced structures [3,4,5,6,7,8,9,10]. Interest in the rheology of micellar solutions is also kindled by their drag-reducing ability and it has been suggested that shear-induced structures play a vital role in this regard [11,12,13]. Despite numerous studies on this subject, however, the origin of the shear-thickening and drag-reduction effect remains unclear.

Recently Liu and Pine [14] reported the formation of shear-induced structures in a CTAB-NaSal micellar solution using a novel direct visualization technique called light scattering microscopy (LSM). In this letter, we exploit LSM to examine the time evolution of shear-induced structures in a different surfactant system and show that there is a strong correlation between the formation of shear-induced structures and the increase in shear and normal stresses under shear flow. This correlation supports the idea of a shear-induced phase transition and provides important dynamical information on how that transition occurs.

Sample and apparatus. – The surfactant system used in this study was tris(2-hydroxyethyl)-tallowalkyl ammonium acetate (TTAA, Ethoquad T/13-50 from AKZO Chemicals, Chicago, USA) and sodium salicylate (NaSal) which forms long worm-like micelles. The rheological properties of this system has been studied extensively because of its practical use as a drag-reducing additive [15,16]. The concentration was 10 mM for both surfactant and counterion, which is high enough to have good optical contrast for making reasonable LSM images but low enough to have a significant shear-thickening effect (at higher concentrations, the shear-thickening is masked by the high equilibrium solution viscosity). A transparent glass Couette flow cell described by Liu and Pine [14] was used for the visualization. The 1-mm gap between

the two concentric glass cylinders (inner cylinder diameter 23.4 mm, outer cylinder rotating) was illuminated by a sheet of light from a laser with the vector normal to the sheet of light pointing in the flow direction. Light scattered from this sheet of light was collected by a CCD video camera so that an image of a flowing region, approximately 1 mm $\times$ 2 mm in size, was formed. Bright regions in the images are produced by higher-than-average fluctuations in the micelle concentration. The shear stress and first normal stress difference were measured with a RMS-800 rheometer equipped with a coni-cylinder flow cell (cup diameter 52 mm, bob diameter 50 mm, bob length 20 mm, and cone angle 0.04 rad). All measurements were performed at a temperature of $22.3 \pm 1°$C.

Results and discussion. – In fig. 1 we show typical LSM images obtained at different times after the commencement of shear flow for $\dot{\gamma} = 60$ s^{-1} for a 10-10 mM TTAA-NaSal sample. The images show a cross-section across the gap of our shear cell. Prior to the commencement of shear flow, scattering from the sample is homogeneous, reflecting the macroscopic homogeneity of the solution, as shown in fig. 1a. Immediately after the commencement of flow, the intensity of the scattered light decreases sharply, as shown in fig. 1b. This initial decrease in the scattering intensity is caused by the stretching of micelles along the flow direction [14]. Sometime after the initial darkening of the images, white structures begin to appear at the inner cylinder and then expand out towards the outer cylinder (fig. 1c-e). The white structure is apparently a new phase produced by the shear. This shear-induced phase (SIP) is more viscous than the unsheared fluid and scatters more light than the unsheared fluid when subjected to stress. Increased light scattering under stress is characteristic of highly crosslinked or entangled systems and has been observed in gels [17,18] and entangled polymer solutions [19,20]. Thus, it seems likely that the SIP is more highly entangled (or crosslinked) than the equilibrium fluid.

It is interesting to note that the SIP appears to grow as densely packed "fingers" which all have approximately the same length. While these finger-like structures appeared in all our measurements in which the SIP was observed, the fingers were not always densely packed but instead often had some finite space, comparable to the width of the fingers, between each finger. Indeed, this is what was reported by Liu and Pine previously in the CTAB-NaSal system [14]. However, we find that over a finite range of concentrations, the fingers are densely packed in our samples. As will become apparent below, this critical feature enables us to compare quantitatively rheological measurements with our LSM visualization measurements and to make some important inferences about the origin of shear-thickening in these solutions.

Continuing our discussion of fig. 1, we see that the new phase continues to grow across the gap until it reaches the outer cylinder (fig. 1e). Once the new phase touches the outer cylinder, the flow becomes chaotic and both dark and bright objects appear (fig. 1f). We believe this is caused by the rupturing and reforming of the SIP which continuously occurs once the new phase spans the gap of the Couette cell.

The main objective of this letter is to compare quantitatively the temporal evolution of the LSM images with rheological measurements of shear thickening in this system. Therefore, in fig. 2, we show a typical rheological curve obtained from the 10-10 mM TTAA-NaSal sample at a shear rate of 60 s^{-1}. After an initial decrease, the first normal stress difference $N_1 \equiv \sigma_{11} - \sigma_{22}$ remains constant for approximately 10 s and then begins to increase. After approximately 160 s, the normal stress reaches a plateau where it fluctuates about an average steady-state level. The shear stress σ_{12} shows qualitatively similar behavior, though noisy signals at low shear rates makes it difficult to accurately determine the time when the shear stress begins to increase. Therefore, we use the normal stress data for our analysis since it is more sensitive to the structural changes than the shear stress data [16]. We note that the rheological behavior,

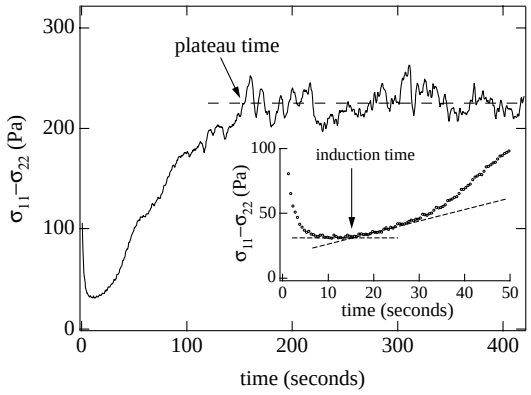

Fig. 2. – Normal stress vs time after the commencement of shear flow. The inset shows how the induction time t_I is obtained from the intersection of two lines. The plateau time t_P is determined by the first crossing of the signal with the average steady-state stress value.

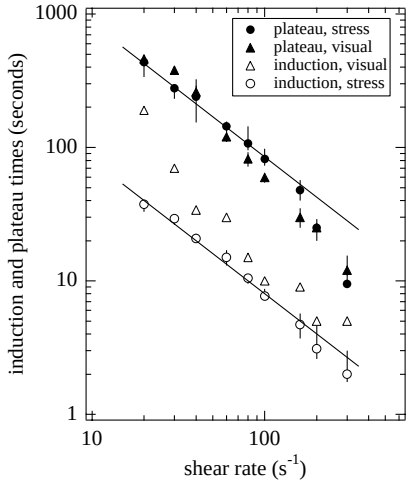

Fig. 3. – Induction times (open symbols) and plateau times (solid symbols) determined by visualization (triangles) and rheological (circles) measurements. Induction and plateau times obtained independently by the two methods are in good agreement. The solid lines have a slope of -1.

as characterized by N_1, bears a remarkable correspondence to the LSM visualization data. The initial decrease in N_1 corresponds to the initial decrease in light scattering intensity. The growth in N_1 corresponds to appearance of the SIP and the saturation in N_1 corresponds to the SIP having filled the gap of the Couette cell. To investigate this correspondence quantitatively, we define an induction time t_I and a plateau time t_P, as shown in fig. 2, consistent with previous rheological research on these systems [16]. While there is some ambiguity concerning how best to define these times, we find that the times vary over a sufficiently large scale that the small differences that result from alternative definitions are completely inconsequential.

To facilitate quantitative comparison between the rheological and LSM data, we have

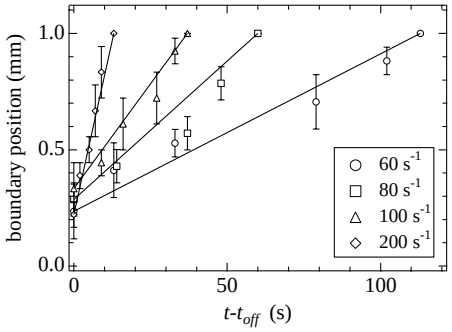

Fig. 4. – Position of the boundary between the SIP and the sheared micellar phase as a function of time for four different shear rates. The error bars indicate the maximum extent of spatial fluctuations in the interface position. For a given shear rate, the velocity of the interface is approximately constant.

measured the time at which the new phase is first visible and the time when it fills the gap for shear rates from 20 s^{-1} to 300 s^{-1}. (Our LSM data do not have sufficient temporal resolution to characterize the initial homogeneous decrease in scattering intensity.) Results are shown in fig. 3. Empty triangles indicate the time t_1 when the first new structure is clearly visible in the gap. Solid triangles indicate the time t_2 when the SIP structure completely fills the gap between the cylinders of the Couette cell. On the same graph we plot the rheological induction and plateau times t_I and t_P obtained independently from the first normal stress measurements. Very similar values of t_P are obtained from our σ_{12} measurements. However, the σ_{12} measurements were too noisy to obtain meaningful values of t_I, as discussed above. The plots reveal a remarkable correspondence between the rheological and structural time scales. The somewhat larger induction time obtained from the LSM than from the N_1 measurements is most likely due to the smaller sensitivity of the visualization technique to the initial formation of the new phase. This is consistent with the suggestion that the intensity of scattering from the SIP is controlled by how strongly it is stretched. When the SIP begins to form, the stresses in the cell are lowest and the SIP is not highly stretched. As the SIP grows across the gap, the stresses increase (fig. 2) and the SIP is more strongly stretched, which increases the intensity of the light scattered from the SIP.

Two conclusions may be drawn from the close correspondence between the data obtained with the two different methods: (1) the induction period t_I, during which there is no measurable increase in stress, corresponds to the period t_1 during which no visible new phase is formed and (2) the temporal increase in stress which occurs between times t_I and t_P corresponds to the growth of a new shear-induced phase across the gap of the shear cell between times t_1 and t_2. The plateau time t_P is the time t_2 when the new structures reach the outer cylinder. Thus, by correlating the images of the temporal evolution of the shear-induced structures with the temporal increase in stress, we identify the shear-thickening transition with the formation of a new shear-induced phase.

We can also examine the rate at which the new phase is formed and its dependence on shear rate. To this end, we show in fig. 4 the position of the front of the new phase as a function of time for four different shear rates between 60 s^{-1} and 200 s^{-1}. The zero position is defined to be at the inner cylinder and the 1-mm position is at the outer cylinder (the width of the gap is 1 mm). The error bars reflect the fact that the front is not perfectly flat. Because the contrast between the SIP and the fluid phase is very low when the SIP is first formed, we

were not able to observe the formation of the SIP at its inception. Thus, the first point at $t - t_{off} = 0$ s is not at the zero position for any shear rate. Nevertheless, fig. 4 shows that the speed at which the interface advances across the cell increases with shear rate. Moreover, within the resolution of our measurements, the speed of the front is approximately constant for a given shear rate.

In summary, we observe a quantitative correlation between the time evolution of the direct visual observations of the inhomogeneous growth of the new shear-induced phase and the measured increase in stress. This correspondence shows that the shear-induced transition is responsible for the shear-thickening in the micellar solution we studied. We suggest that this shear-induced transition is also the mechanism for the similar rheological behavior observed in many other surfactant systems.

***

P.B. wishes to thank the CNRS for partial financial support. We also acknowledge support by the MRL Program of the National Science Foundation under Award No. DMR96-32716. We that AKZO Chemicals for providing the surfactant TTAA.

REFERENCES

[1] T. Nash, *Nature*, **177** (1956) 948.
[2] S. Gravsholt, *Proc. Int. Congr. Rheol.*, **8** (1980) 629.
[3] H. Rehage and H. Hoffmann, *Rheol. Acta*, **21** (1982) 561.
[4] I. Wunderlich, H. Hoffmann, and H. Rehage, *Rheol. Acta*, **26** (1987) 532.
[5] J. Kalus, H. Hoffmann, S.-H. Chen, and P. Lindner, *J. Phys. Chem.*, **93** (1989) 4267
[6] S.Q. Wang, *J. Phys. Chem.*, **94** (1990) 8381
[7] S. Hofmann, A. Rauscher, and H. Hoffmann, *Ber. Bun. Ges.*, **95** (1991) 153.
[8] M.S. Turner and M.E. Cates, *J. Phys., Condens. Matter.*, **4** (1990) 3719
[9] R. Bruinsma, W.M. Gelbart, W.M., and A. Ben-Shaul, *J. Chem. Phys.*, **96** (1990) 7710
[10] Y. Hu, S. Q. Wang, and A. M. Jamieson, *J. Rheol.*, **37** (1993) 531.
[11] A. V. Shenoy, *Coll. Poly. Sci.*, **262** (1985) 319.
[12] H.-W. Bewersdorff, B. Frings, P. Lindner, and R. C. Oberthur, *Rheol. Acta*, **25** (1986) 642.
[13] D. Ohlendorf, W. Interthal, and H. Hoffmann, *Rheol. Acta*, **25** (1986) 468.
[14] C.-h. Liu and D. J. Pine, *Phys. Rev. Lett.*, **77** (1996) 2121.
[15] S. Hofmann, P. Stern, and J. Myska, *Rheol. Acta*, **33** (1994) 419.
[16] Y. Hu and E. F. Matthys, *Rheol. Acta*, **35** (1996) 470.
[17] A. Ramzi *et al.*: , *J. Phys. IV (France)*, **3** (1993) 91.
[18] C. Rouf *et al.*: , *Phys. Rev. Lett.*, **73** (1994) 830.
[19] X.-l. Wu, D. J. Pine, and P. K. Dixon, *Phys. Rev. Lett.*, **66** (1991) 2408.
[20] J. W. van Egmond, D. E. Werner, and G. G. Fuller, *J. Chem. Phys.*, **96** (1992) 7742.